NOTICE CONCERNING COPYRIGHT RESTRICTIONS

This document may contain copyrighted materials. These materials have been made available for use in research, teaching, and private study, but may not be used for any commercial purpose. Users may not otherwise copy, reproduce, retransmit, distribute, publish, commercially exploit or otherwise transfer any material.

The copyright law of the United States (Title 17, United States Code) governs the making of photocopies or other reproductions of copyrighted material.

Under certain conditions specified in the law, libraries and archives are authorized to furnish a photocopy or other reproduction. One of these specific conditions is that the photocopy or reproduction is not to be "used for any purpose other than private study, scholarship, or research." If a user makes a request for, or later uses, a photocopy or reproduction for purposes in excess of "fair use," that user may be liable for copyright infringement.

This institution reserves the right to refuse to accept a copying order if, in its judgment, fulfillment of the order would involve violation of copyright law.

Geothermal Resources Council TRANSACTIONS, Vol. 14, Part II, August 1990

THREE-DIMENSIONAL INVERSION OF TELESEISMIC TRAVEL TIMES FOR VELOCITY STRUCTURE IN THE LARDERELLO GEOTHERMAL FIELD, ITALY

John E. Foley [1] M. Nafi Toksöz [1] Fausto Batini [2]

(1) Earth Resources Laboratory, Massachusetts Institute of Technology, Cambridge, MA.
(2) Ente Nazionale per l'Energia Elettrica (ENEL), Larderello, Italy

ABSTRACT

The analysis of teleseismic travel time residuals observed on the Larderello Seismic Network of central Italy has revealed a sharp low velocity zone in the center of the geothermal production area. Residuals from 101 teleseismic events, automatically determined with the implementation of a simulated annealing optimization procedure, are inverted to produce an image of an anomalous body interpreted to be an intrusive heat source. The top of this body is constrained to be below 6 km depth from local earthquake seismicity patterns and extends to a depth of greater than 20 km. The intrusive body broadens with increasing depth and may extend into the upper mantle. The observed travel time residual anomaly corresponds with observed gravity lows, high heat flow, the shallowing of a dominant upper-crustal reflection, and diminished teleseismic P-wave amplitudes. This body has elevated the temperatures in the region to over 350 degrees C at 2 km and is the origin of the geothermal energy.

Introduction

The deep structure of the Larderello Geothermal Field of Central Italy is investigated by inversion of teleseismic travel time residuals. The information this study provides is necessary to further the basic understanding of the origin of the geothermal phenomenon observered in Larderello. We determine the size, extent and magnitude of the low velocity zone (LVZ) within the geothermal region which gives rise to the observed teleseismic travel time anomalies, temperature anomalies, gravity anomalies, P-wave teleseismic amplitude anomalies and variation in depth of a key crustal reflection horizon observed in the region. This information helps us understand the regional processes which control this important economic resource.

A wide range of studies of Earth velocity structure in volcanic regions utilizing anomalous travel times and amplitudes of seismic waves have been made, examples include Hawaii (Ellsworth, 1977), Yellowstone (Iyer, et. al, 1981), The Geysers (Oppenheimer et. al, 1981) and Long Valley, California (Sanders, 1984). See Iyer (1988) for a review.

Geologic Background

Most Italian geothermal areas are located, from the geological point of view, in the complex structures of the Apennines, which are tectonically characterized as overlapping folds Boccaletti at al., 1983). The inner Apennines are characterized by high heat flow. The Bouguer anomalies and the data from deep seismic soundings show a thin crust with a Moho discontinuity at a depth of less than 20 km and a soft mantle (Vp=7.8 km/sec) (Giese et al., 1981). Moreover, tensile stresses are present in the area and caused the rise of hot masses from the mantle into the crust.

This geological/structural evolution gave rise to a local geothermal anomaly with heat flow values exceeding 300 mW/m2 in correspondence to the largest geothermal fields. The Larderello field is a system of the hydrothermal type, and is the most important in Italy, with an installed capacity of over 550 MWa. The cap rock is represented by sedimentary terrains (clays and conglomerates) deposited during the post-orogenic transgressive phase and a complex of tectonic wedges composed of mainly clayey and arenaceous flysches. The complexes overthrusted during the Alpine orogeny onto other tectonic wedges made up intensely fractured Triassic evaporites (chiefly dolomitic limestones and anhydrites) which represent the main reservoir exploited so far.

A tectonic surface separates the complexes and tectonic wedges from a crystalline basement including formations characterized by an increasing degree of metamorphism towards the bottom, with the phyllites and quartzites giving way to micaschists and gneisses. The recognition of the structural boundaries of the main units was made possible by the seismic reflection data, which were compared with results from field geology and wells drilled in the areas of question.

Well defined on nearly all reflection lines are some deep markers, sufficiently continuous and with clear amplitude and frequency characters. Horizon K has been followed in correspondence to these markers. It follows the major amplitude events and rests on a group of reflectors which are mostly parallel to it. The structural trend of K generally reflects the structural behavior of the top of the metamorphic basement, with a main positive element placed in a roughly NNE-SSW direction. The minimum depth (about 3000 m) are observed in proximity to the San Pompeo 2 well, between seismic stations LAGO and FRAS. The structural panorama is complicated by vertical discontinities, well evidenced on the seismic sections, which in general determine the dipping nature of the K horizon at the boundaries of the areas now being explored. As far as the nature and the causes of the K reflections are concerned (Batini and Nicolich, 1984), it should be stressed once again that they are determined by strong variations of the reflection coefficient and thus by the presence of a medium of a very different acoustic impedance from that of the embedding medium.

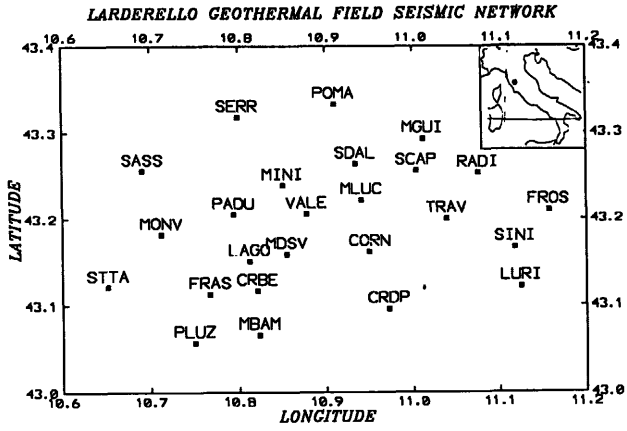

Figure 1: ENEL seismic network, located in Central Italy, was established in 1985 has 26 uniform and calibrated stations.

Inside the crystalline basement, strongly corrugated during the Hercynian orogenesis and subsequently subjected to tensile stresses caused by the rise of intrusive bodies during the late Alpine orogenic phase, densely fractured permeable zones are present which allow circulation of the geothermal fluids (Batini et al., 1985; Batini et al., 1988).

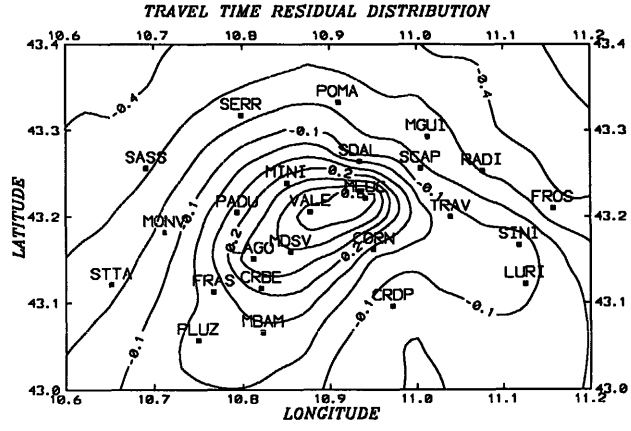

Figure 2: Average travel time residuals recorded on the Larderello seismic network from all 101 events. All residuals represent data reduced to 6 km. Contours are lines of equal residual plotted at 0.1 second intervals. See text for description of the residual patterns. Station names are included for reference.

Data

The data for the teleseismic travel time inversion and the P-wave amplitude anomaly calculations come from the Italian National Energy Board (ENEL) seismic monotoring network located in Larderello, Italy (Figure 1, and Table 1). This seismic network began recording digital seismic data in 1985 and has recorded approximately 200 teleseismic events through June, 1988. The network covers an area approximately 30 km by 40 km and has 26 uniform and calibrated stations with 1 Hz vertical geophones (Batini et al., 1985). The average station spacing is 6.5 km. Of 200 teleseismic events, 101 selected on the basis of high quality, were chosen for analysis. Events with waveforms that have emergent onsets which makes accurate timing of the arrival at each station very difficult, and events recorded on less than 15 stations were not included.

A waveform correlation procedure based on the simulated annealing technique (Rothman, 1986) was applied to the data in order to automate the travel time residual calculations and to make more quantitative classifications of the quality of arrival time pick. After a set of relative travel times are determined, we calculate the relative travel time residuals with respect to a Herrin Earth model. In addition to elevation corrections, we further reduce to data to a depth of 6 km. We lower the reference datum deeper into the crust to reduce upward smearing of residuals into the top layers of the model from the strong, deeper anomalies below. Analysis of the distribution of the deepest Earthquakes in the region indicates that Earthquakes are occurring across the entire network to a depth of at least 6 km, justifying the datum level reduction. This reduction was accomplished by utilizing the well defined near surface velocity structure determined from the extensive reflection work done in the region (Batini and Nicolich, 1984). Once the corrections are applied to the travel times the absolute residuals are calculated using a standard process common to most teleseismic travel time inversions procedures, see Zandt (1981) for complete details.

Travel time residuals were calculated for 101 teleseismic Earthquakes and nuclear explosions. Gaps in coverage are quite large from the SW (74 degrees); however, there is sufficient azimuthal variation in the data to obtain a varied crossfire of rays through the model.

Figure 2 shows the average station travel time residuals for all of the data, and from this map we see that the strongest low velocity area is concentrated in the center of the network. Strong positive residuals (slow) of up to 0.6 sec are observed which contrast to the negative (fast) residuals up to -0.4 sec on the periphery. The contour of zero residual is aligned to the NE with dimensions of approximately 30 by 40 km. The total travel time differences are about 1.0 second which represents a very strong travel time anomaly for a small region (approximately 25 km between average extremes). This range in average travel time residual is similar to those found in Geysers – Clear Lake Geothermal field in California, (Oppenheim et al., 1981).

To produce a one second relative delay for a near vertical ray from crustal effects requires a 35 percent velocity decrease along the entire crustal raypath. Velocities of rhyolite melts (Murase and McBirney, 1973) and dacite melts (Hayakawa, 1957) of about 4 km/sec would represent a 38 percent velocity reduction of a 6.5 km/sec country rock. This indicates that the low velocity anomaly either exists as a large body of melted magma in the crust or, more likely, that it penetrates the crust into the mantle to depths below 20 km.

Patterns exhibited in Figure 2 indicate that average station travel time residuals calculated for events with rays passing through the center of the network have generally slower raypaths. Those paths which exclude the network center are generally faster. When stations located near the zero-second contour are examined in detail, we see this effect clearly and can conclude that the lateral changes in velocity are abrupt.

Inversion

Travel time residuals are inverted for velocity perturbations using the method of Aki et al.(1977) This method of inversion has been used quite extensively in the past, particularly for the purposes of magma chamber delineation. See Iyer(1988) for a review of Aki inversions in volcanic regions. The details of the inversion are only sketched below, for a complete review of the inverse formulation see Zandt (1978), or Taylor and Toksoz (1979).

An Earth model consisting of a set of layers subdivided into right rectangular blocks is established as a starting model. For each event and each station, rays are traced through the model. Travel time residuals are distributed in the blocks along the raypath proportional to the length of the ray in each block. Since events are located are various distances and azimuths from each station, a dense mesh of distributed residuals is formed beneath the network. The Aki technique solves the system of equations which characterizes this travel time distribution using a damped least squares technique.

The starting model for the travel time inversion is the five layer model in which the crust is characterized by three layers each of which is 5 km thick with velocities of 6.5, 7.0, and 7.5 km/sec, respectively. The upper mantle is parameterized by two 10 km thick layers at 8.0 km/sec. This model is consistent with deep reflection work done in Larderello (Batini et al., 1988) and the refraction model of Giese et al., (1981) of central Italy.

Discussion

Figure 3 shows the results of the travel time inversion. These plots show the velocity perturbation for each of the five layers in percent of the background velocity as contours of equal velocity perturbation. For the crustal layers (1, 2, and 3; from 6 to 21 km) the region of low velocity is confined to the center of the network in an area 25 by 40 km in extent, with an elongate pattern to the NE. This pattern coincides with the region of low amplitude teleseismic P-waves, high heat flow, negative Bouguer gravity anomaly, and the elevated **K** reflection horizon and will be discussed below.

Layers 4 and 5 (depth from 21 to 41 km) also have a distinct low velocity pattern in the center of the network. The relative velocity perturbations are still quite large at these depths (10 percent in the center). The zone of maximum low velocity migrates to the northeast at greater depths and the total area of LVZ increases. Slices through the final perturbed model (Figure 4) show the pattern of the anomalous body in vertical cross section. Velocity contrasts are depicted with different shade patterns with cross hatched blocks representing velocity decreases and stippled blocks representing regions of increased velocity. Blocks without any pattern represent regions not sampled densely enough (at least 10 rays) for a parameter estimate to be made.

The SW to NE slice (Figure 4, left) shows that strong velocity reductions (to 18 percent) are necessary to satisfy the data from depths of about 6 to 16 km. The LVZ in the crustal

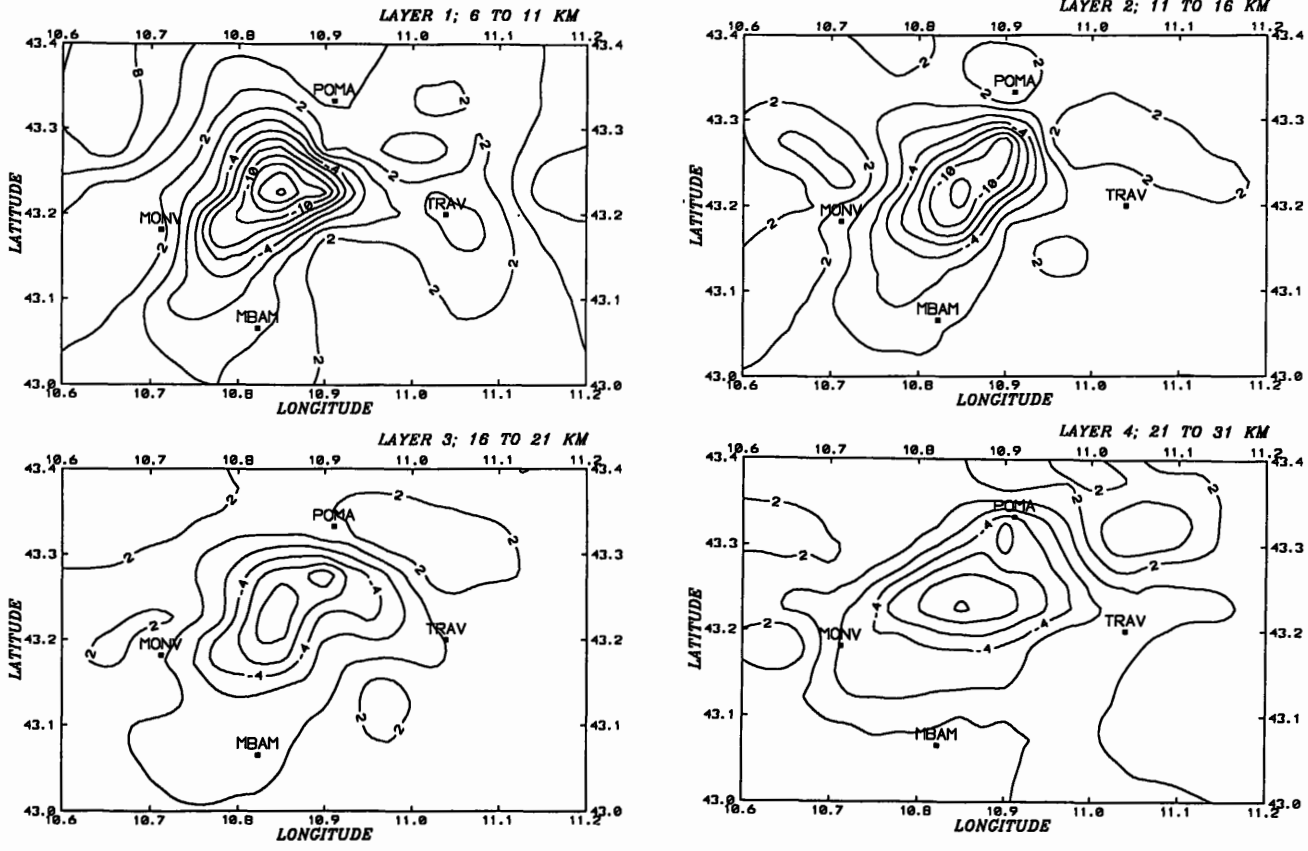

Figure 3: Inversion results for Layer 1 through Layer 4. Plotted are contours of equal velocity perturbation (from starting velocity; see text) at an interval of 2 percent. We see a strong localized anomaly in the center which is about 25 km in diameter.

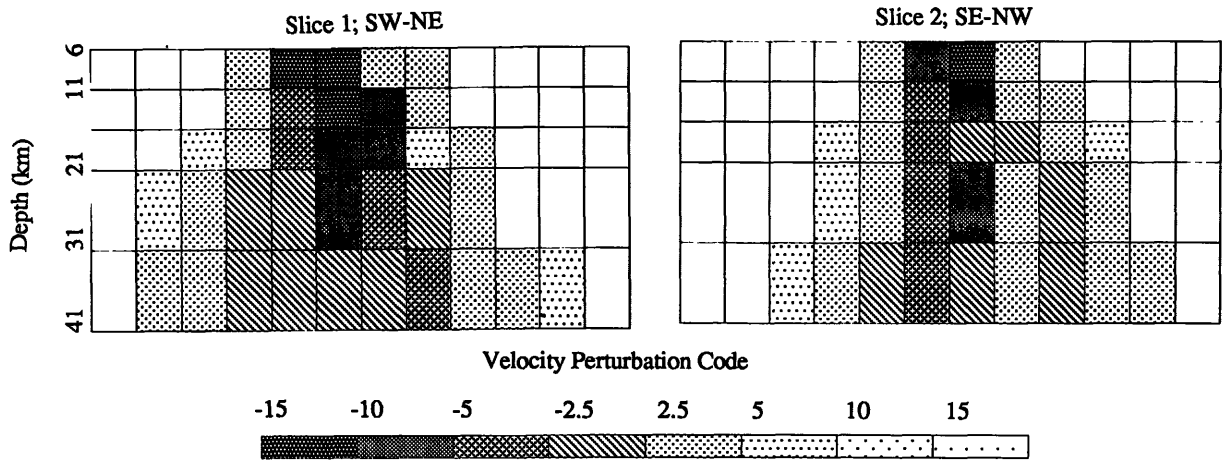

Figure 4: Inversion results plotted as vertical slices through the region. Diagonal slices from SW to NE (left) and NW to NE (right). All block widths are 7 km. The three crustal layers are 5 km thick and the two mantle layers are 10 km thick. The top of the model represents a depth of 6 km below the surface. The velocity perturbation code is relative to the starting model described in text.

Station Name	Lat	Lon	Elev m	Resid sec	Temp deg C	K m	Grav mGal	Amp percent
MINI	43.23	10.85	444	0.37	260	4600	19	0.33
SERR	43.31	10.79	223	-0.23	150	—	26	2.60
POMA	43.33	10.90	231	-0.19	150	—	33	1.94
SDAL	43.26	10.93	380	-0.13	225	5000	23	0.22
SCAP	43.25	11.00	360	-0.25	175	8000	24	0.21
MGUI	43.29	11.01	341	-0.26	150	—	31	0.44
RADI	43.25	11.07	489	-0.30	150	8500	29	0.22
MLUC	43.22	10.94	572	0.83	240	4200	21	0.10
FROS	43.20	11.15	432	-0.38	150	—	26	0.92
SINI	43.16	11.11	350	-0.03	150	—	16	1.08
LURI	43.12	11.12	458	-0.08	150	—	18	1.09
TRAV	43.19	11.03	472	-0.05	300	7000	17	1.12
CORN	43.16	10.94	886	-0.03	250	4400	24	0.64
VALE	43.20	10.87	782	0.63	320	3800	20	2.01
CRDP	43.09	10.97	816	-0.21	150	—	18	0.62
MDSV	43.15	10.85	754	0.51	300	3600	19	0.56
CRBE	43.11	10.82	442	0.08	300	3200	25	0.99
MBAM	43.06	10.82	342	-0.03	250	3400	32	0.80
LAGO	43.15	10.81	319	0.40	300	3000	15	2.21
PADU	43.20	10.79	439	0.16	250	4600	22	0.26
SASS	43.25	10.69	438	-0.33	150	—	40	1.11
MONV	43.18	10.71	445	-0.20	255	5000	29	0.68
FRAS	43.11	10.76	220	0.00	200	4000	30	0.64
STTA	43.12	10.65	361	-0.28	150	—	37	0.55
PLUZ	43.05	10.74	156	0.00	150	4000	33	1.04

Table 1: Parameter Values from the Larderello Geothermal Field Seismic Network

part of the model is about 20 km wide. Deeper in the crust and in the upper mantle, the perturbations are smaller and cover a larger region. However, the results in the lower part of the model may be corrupted by smearing effects in the inversion. The residual redistribution technique tends to back propagate travel time residuals equally along each raypath. When criss-crossing ray coverage is not sufficient in an area, artificial velocity anomalies can be created. This effect may be accentuating the deep and widespread low velocity area of layers 4 and 5 where velocity reductions of up to 10 percent are required by the data, and the LVZ covers an area about 35 km wide. The NW to SE slice shows a more uniform pattern of low velocity, with a reduction of about 10 percent existing from the top layer (6 km) to a depth of 41 km. The width of the LVZ is about 15 km in the crustal layers, and increases at depth. However, resolution of the LVZ is poor to the SE due to poor data coverage.

The anomolous body which gives rise to the velocity structure discussed above also has strong effects on other geophysical observations made in the region. The temperature field measured at 2 km (Figure 5a), Bouguer gravity field (Figure 5b), average teleseismic body wave amplitudes (Figure 5c), and the depth to the K reflection horizon (Figure 5d) are strongly variable across the network. See Table 1 for parameter estimates at each station. The 2-km temperature values vary from about 150 to 350 degrees with the highest values in the center of the field corresponding with an area of very active geothermal production. The Bouguer gravity anomaly (Cataldi, 1978) is also greatest in the center of the field, with a gavity low of 25 mGals. A low density, silica-rich magmatic intrusion has been proposed to be the source of this gravity feature (Puxeddu, 1984). This gravity feature compares well with gravity lows of 30 mGals at The Geysers (Iyer, 1984) and 50 mGals at Yellowstone (Ellsworth, 1977).

The depth of the K reflection horizon (Batini, 1988) which varies in depth from about 3 to 8 km, is deepest on the periphery of the network and shallowest in the center of the network coincident with the area of high geothermal activity. Teleseismic P-wave amplitude residuals patterns can be used to help understand the structure beneath seismic arrays (Thompson and Gubbins, 1982). Relative amplitude residuals were calculated for all events used in the travel time residual calculations using the formula

$$A(i) = \frac{1}{N}\left(\sum_{i=1}^{N} \frac{SWP}{AWP}\right) \quad (1)$$

Where SWP is the station window power for an individual event, AWP is the average window power for the event, and N is the number of events recorded at the station. Window power

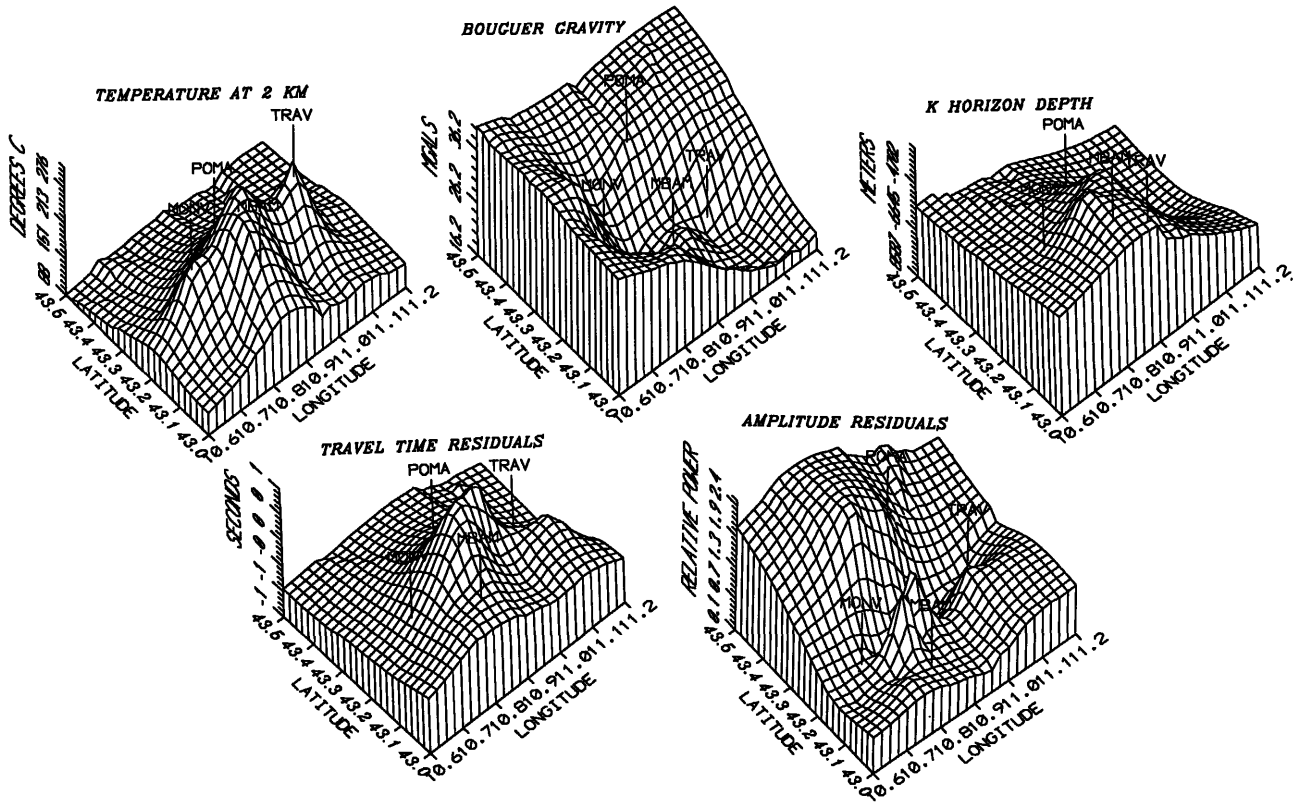

Figure 5: Geophysical parameter maps of data recorded within the Larderello geothermal field. Clockwise from upperleft; Temperature measured at 2 km in degrees C, Bouguer Gravity anomalay in mGals, Depth to the K reflection Horizon in meters, Teleseismic amplitude residuals from direct arrival measurements and Average travel time residuals.

is defined as the sum of the squared amplitudes in the first 1 second of the event. The average amplitude residual variations for the PKIKP events (Figure 5e) show a complicated pattern with generally smaller window power values in the center of the network and larger values to the North.

To view the correspondence of various geophysical parameters we calculated non-dimensionalized product maps (Davis, 1973). These maps are made by first converting the single parameter maps into standard maps such that each point represents the variation of the parameter from the average value weighted by the data standard deviation. The final maps are made from point–by–point multiplication of two standard maps. Two non-dimensionalized product maps are shown in Figure 6. The first shows the correspondence between travel time residuals and temperature, with only PKIKP events used in the calculations to reduce the effect of gaps in the azimuthal data coverage. Two phenomena are visible on this map, the first of which clearly shows that the highest temperatures directly correspond with the most delayed PKIKP travel times. The peak is centered near station VALE.

The second observation is that directly to the west and east of the peak correspondence, we see distinct lows in the non-dimensionalized product which come from high temperatures which correspond geographically with normal to fast PKIKP travel time averages. This tells us that the anomalous body, which gives rise to the travel time delays and high temperatures in the center of the network, only effects the temperature observations on the periphery and not the travel times. This may represent a region of very hot but still competent rock.

The product map between PKIKP travel times and averaged relative PKIKP amplitude anomalies (Figure 5, right) shows a complicated pattern of correspondence. Here, the sense of the amplitude residuals is reversed to produce a positive value when large amplitudes and delayed amplitudes match. From this map we can see that, in the center of the network, smaller than average amplitudes and low velocity regions coincide. To the northwest, larger than average amplitudes and relative high velocities correlate. This leads us to believe that the existence of a magma chamber in this area is either scattering or attenuating energy to diminish the average window power calculations made in the region of low velocity. Very low Q values may exist in fully melted regions and significantly reduce amplitudes provided that ray travels in the material for a few wavelengths. A high degree of scattering may also exist in the region due to the large velocity and density contrasts between the competent country rock and partially of fully melted material. Forward modeling of the waveshapes and amplitudes is necessary to separate these factors.

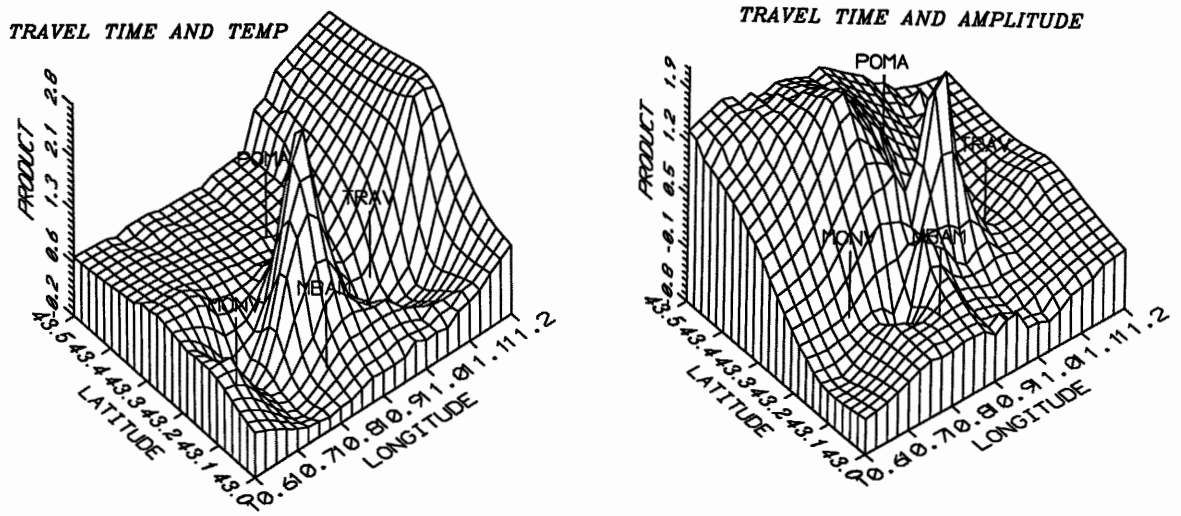

Figure 6: Non-dimensionalized product maps made by point–by–point multiplication of two Standard maps; Travel time residual and temperature (left) and Travel time residuals and teleseismic P-wave amplitude residuals (right).

Summary

Our interpretation of the geophysical data described above is that a magma chamber exists beneath the geothermal field in Larderello, Italy. Travel time inversion of relative teleseismic P-wave delays reveal a roughly cylindrical low velocity body with a diameter of about 15 to 20 km. Given the high temperatures at 2 km (up to 350 degrees), it is believed that this LVZ may exist as a complex volume of partially or fully melted rocks with a bulk velocity reduction of 15 to 20 percent in the crust.

The depth of the top of this region is assumed to be below the level of active seismicity at a depth of 6 km. Tomographic inversion of travel time residual data indicates clearly that the LVZ penetrates to a depth of at least 21 km and strongly suggests that the region extends deeper into the upper mantle to a depth of at least 40 km. At depth the zone trends to the northeast and broadens to a width of about 40 km.

The K horizon, which is characterized by a strong reflection at depths between 3 km in the center of the network to 7 or 8 km on the periphery, may represent a petrophysical boundary (Batini, 1988) marking a highly fractured, fluid-filled region which resulted from the high stresses induced from the magmatic implacement of a low density, silica-rich molten material (Giese et al., 1981). High-angle normal faults on the K horizon, seen on many reflection lines and interpreted from local earthquake fault mechanism analysis (Batini et al., 1985), are consistent with this model.

References

Aki, K., Christoffersson, A. and Husebye, E.S., Determination of the three-dimensional seismic structure of the lithosphere, J. Geoph. Res., 82, 237-296, 1977.

Batini, 1988

Batini, F. and Nicolich, R., The application of seismic reflection methods to geothermal exploration, Seminar on Utilization of Geothermal Energy for Electric Power Productio and Space Heating, 11–17 May, Florence, 1984.

Batini, F., Console, R. and Luongo, G., Seismological stud of Larderello–Travale geothermal area, Geothermic,s 14, 255 272, 1985.

Boccaletti, M., Coli, M., Eva, C., Ferrari, G., Giglia, G. Lazzarotto, A., Merlanti, F., Nicolich, R., Papani, G., an Postpischl, D., Considerations on the seismotectonics of th northern Apennines, Tectonophysics, 47, 1983.

Cataldi, R., Lazzarotto, A., Muffler, L. P. J., Squarci, P. Stefani, G. C., Assessment of geothermal potential of centra and southern Tuscany, Geothermics, 7, 91-131, 1978.

Davis, J.C., Statistics and Data Analysis in Geology, Joh Wiley and Sons, 550 pp., 1973.

Ellsworth, W. L., Three dimensional structure of the crus and upper mantle beneath the island of Hawaii, Ph.D thesi Massachusetts Institute of Technology, 377 pp., 1977.

Giese, P., Morelli, C., Nicolich, R., and Wigger, P., Seismis che Studien zur Bestimmung der Krustenstruktur im Bereic der geothermischen anomalie der Toskana, Commission of th European Communities, EUR 75-78 de MF, 1981.

Thompson, C. J., and Gubbins, D., Three-dimensional lith spheric modeling at NORSAR: linerarity of the method an amplitude variations from the anomalies, Geophy. J. Roy Ast. Soc., 71, 1-36, 1982.

Hayakawa, M., Prospecting of the underground structure a "Showa-Shinzan" by various geophysical methods, particularl seismic survey, Jpn. J. Geophy., 1, 13-20, 1957.

Herrin, E., 1968 seismological tables of P-phases, Bul Seis. Soc. Amer., 58, 1193–1241,1968.

Iyer, H. M., Seismological detection and delineation of mag chambers beneath interplate volcanic centers in western U.S.A in Modeling of Volcanic Processes, King, C., and Scarpa, F editors, Friedr. Vieweg and Sohn, 1988.

Iyer, H. M., Geophysical evidence for the locations, shape and sizes and internal structures of magma chambers beneat region of Quaternary volcanism, Phil. Tran. R. Soc. Londor Ser A, 310 473-510, 1984.

Murase, T., and McBirney, A, R., Properties of some common igneous rocks and their melts at high temperatures, Geol. Soc. Amer. Bull., 84, 3563-3592, 1973.

Oppenheimer, D. H., and Herkenhoff, K. E., Velocity–density properties of the lithosphere from three-dimensional modeling at The Geysers-Clear Lake region, California, J. Geophys. Res., 86, 6057-6065, 1981.

Puxeddu, M., Structure and late Cenozoic evolution of the upper lithosphere in southwest Tuscany (Italy), Tectonophysics, 101, 357-382, 1984.

Rothman, D., Automatic estimation of large residual statics corrections, Geophysics, 51, 332-346, 1986.

Sanders, C. O., Location and configuration of magma bodies beneath Long Valley California, determined from anomalous Earthquake signals, J. Geophys. Res., 89, 8287-8302, 1984.

Taylor, S. R., and Toksoz, M. N., Three dimension crust and upper mantle structure of the northeastern United States, J. Geophys. Res., 84, 7627-7644, 1979.

Zandt, G., Study of the three dimensional heterogeneity beneath seismic arrays in central California and Yellowstone, Wyoming, Ph.D. thesis, Massachusetts Institute of Technology, 1978.

cm to dm thick, in a dacitic tuff-breccia. The lost circulation zones at these depths were plugged after pumping cement (42 bags) downhole.

Drilling continued to a depth of 87.45 m, with PQ-size and was cased to that depth with HW casing. At 87.45 m the blow-out preventer was installed and tested. From a depth of 87.45 m to about 700 m, HQ size drill rods were used. The coring operations to t.d. were relatively uneventful and recovery of >95% core was made at an average rate of 20 m per day.

Preliminary interpretation of the core suggests that the thin edge of the Ixpaco phreatic tuff ring, dated at 2900 years, was reached at a depth of 65 m. Overlying the ring is a lobe of an avalanche breccia from the nearby Peña Blanca dacite dome. Below the tuff ring, from a depth of 66.5 m to 144.6 m, is a section of tuff-breccia with pumiceous dacite clasts, believed to be from an eruption that preceded the emplacement of the Peña Blanca dome; this deposit is hydrothermally fractured and intensely altered at three levels (Fig. 2), possibly by the phreatic explosions that formed the nearby Laguna Ixpaco crater.

From depths of 144.6 m to a fault contact at 253.75 m is a unit interpreted by G. Heiken to be massive tuff. The "tuff unit" is welded in part, with chloritic and hematitic alteration. Possibly this tuff is the pyroxene andesite ignimbrite, which is correlated with the Qai tuff deposits of Duffield *et al.* (1989) and dated at 38,300 years.

Below 253.75 m, to a depth of about 700 m (at the time of this writing), are interbedded andesitic lavas, scoria, thin tuff beds, and laharic breccias of the Miraflores composite cone (Qam unit of Duffield *et al.*, 1989) (Fig. 2). This andesitic sequence, mostly lavas, is intensely chloritized, with very low permeability; nearly all pore space is filled with hydrothermal minerals. At the time of this writing, the last rocks penetrated were faulted, with some open veins present.

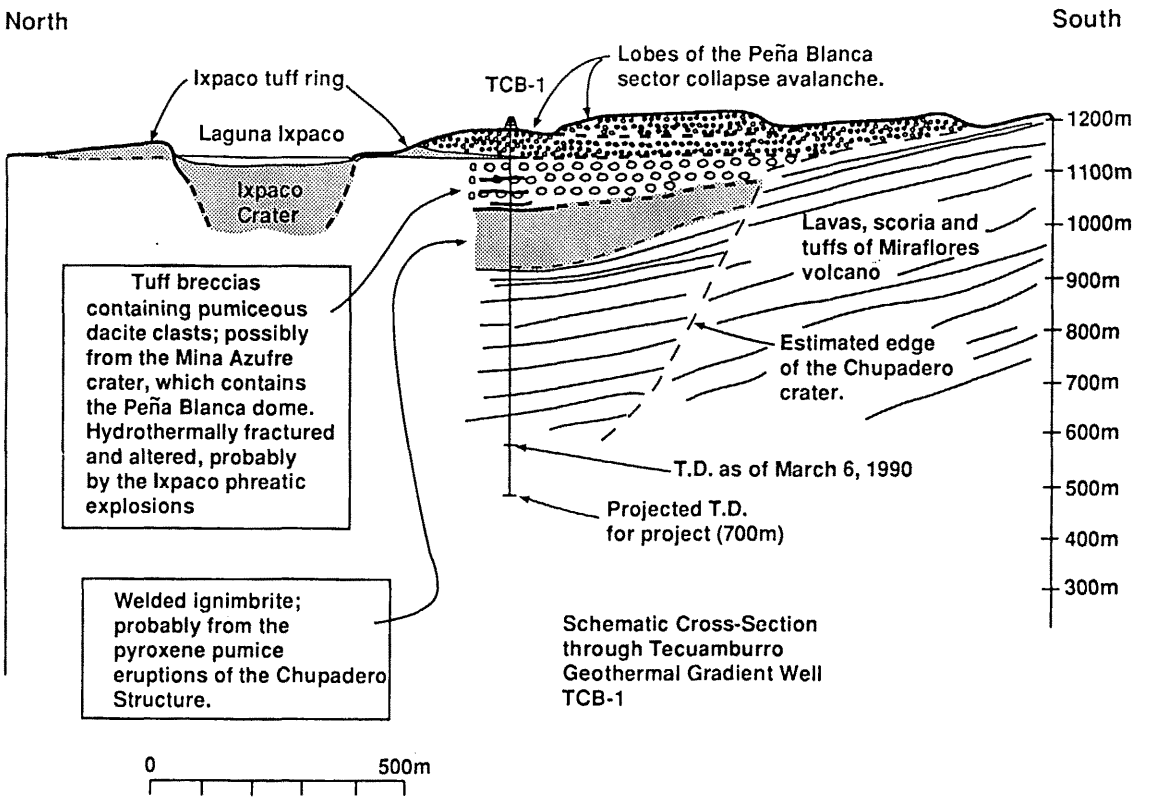

Figure 2. Schematic north-south cross-section through Tecuamburro geothermal area geothermal gradient well TCB-1. Elevations are above mean sea level. No vertical exaggeration. Geologic interpretation represented on this section is from G. Heiken.

TEMPERATURE GRADIENT

At a depth of 400 m, a temperature log was made with a Kuster[tm] tool. Below that depth, measurements with maximum-reading thermometers were made every 50 m. The unequilibrated thermal gradient is 38.4°/100 m (Fig. 3). The core hole will be logged one week after this paper is due and the results will be presented at the GRC meeting in August, 1990.

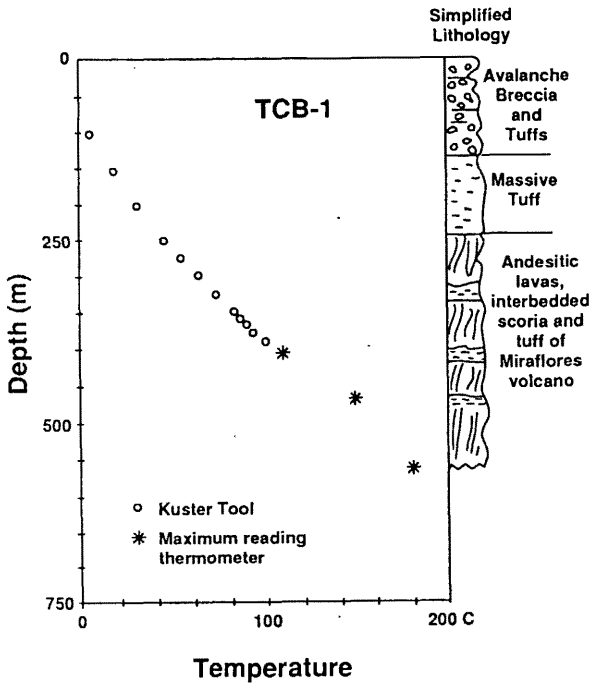

Figure 3. Unequilibrated temperature log and preliminary lithologic interpretation of geothermal gradient well TCB-1.

CONCLUSIONS

We are drilling the first geothermal gradient core hole, TCB-1, in the Tecuamburro geothermal area, Guatemala to test hypotheses developed during the prefeasibility studies (Duffield *et al.*, 1989; Goff *et al.*, 1989): (1) The presence of a massive, partly-welded 110-m-thick tuff sequence at depth (if verified) would confirm the existence of the 4-km-diameter Chupadero crater, which, as a small caldera, could be an excellent heat source. The tuff sequence may also serve as a caprock. (2) Alternatively an unequilibrated thermal gradient of 38.4°C/100 m supports the gas geothermometer temperatures of about 300°, determined at the nearby Laguna Ixpaco phreatic crater and acid lake. The striking similarity in gas compositions between fumaroles at Laguna Ixpaco and fumaroles at the summit of Tecuamburro suggests that the geothermal reservoir may be centered beneath the main volcanic ediface. Integration of results from TCB-1 with previous studies is intended to provide the Guatemalan government with information for planning the next phase of the geothermal assessment of the Tecuamburro site.

ACKNOWLEDGEMENTS

The authors wish to thank E. VanEeckhout, and S. Booth (Los Alamos National Laboratory), C. Duisberg and M. Funes (Regional Office, Central American Project, USAID), and A. Caicedo (INDE), for their organizational work that made this project possible. We also thank the Swissboring drilling crew, whose professional efforts made a difficult job look easy. This project is funded by the U.S. Agency for International Development, under the auspices of the U.S. Department of Energy.

REFERENCES

Duffield, W. A., Heiken, G. H., Wohletz, K. H., Maassen, L. W., Dengo, G., and McKee, E. H., 1989, Geology and geothermal potential of the Tecuamburro Volcano area of Guatemala: *Geotherm. Resourc. Counc. Trans.* **13**: 125.

Goff, F., Truesdell, A. H., Janik, C. J., Adams, A., Roldan-M, A., and Meeker, K., 1989, Hydrogeochemical exploration of the Tecuamburro Volcano region, Guatemala: *Geotherm. Resourc. Counc. Trans.* **13**: 141.

Heiken, G. and Duffield, W., eds., 1989, An evaluation of the geothermal potential of the Tecuamburro Volcano area of Guatemala: Los Alamos Nat. Lab. Report (in press; open-file report LA-UR-89-2973, available on request): 110 pp.